

Article

Optimal Homotopy Asymptotic Method for an Anharmonic Oscillator: Application to the Chen System

Remus-Daniel Ene ^{1,*}  and Nicolina Pop ^{2,†} 

¹ Department of Mathematics, Politehnica University of Timisoara, 2 Victoria Square, 300006 Timisoara, Romania

² Department of Physical Foundations of Engineering, Politehnica University of Timisoara, 2 Vasile Parvan Blvd, 300223 Timisoara, Romania

* Correspondence: remus.ene@upt.ro

† These authors contributed equally to this work.

Abstract: The aim of our work is to obtain the analytic solutions for a new nonlinear anharmonic oscillator by means of the Optimal Homotopy Asymptotic Method (OHAM), using only one iteration. The accuracy of the obtained results comes from the comparison with the corresponding numerical ones for specified physical parameters. Moreover, the OHAM method has a greater degree of flexibility than an iterative method as is presented in this paper. Based on these results, the analytically solutions of the Chen system were obtained for a special case (just one analytic first integral). The chaotic behaviors were excluded here. The provided solutions are usefully for many engineering applications.

Keywords: ordinary differential equations; solution of equations; Chen system; anharmonic oscillator; approximate solution

MSC: 34C14; 37M05; 37M99; 37N99



Citation: Ene, R.-D.; Pop, N. Optimal Homotopy Asymptotic Method for an Anharmonic Oscillator: Application to the Chen System. *Mathematics* **2023**, *11*, 1124. <https://doi.org/10.3390/math11051124>

Academic Editor: Nicolae Herisanu

Received: 25 January 2023

Revised: 14 February 2023

Accepted: 22 February 2023

Published: 23 February 2023



Copyright: © 2023 by the authors. Licensee MDPI, Basel, Switzerland. This article is an open access article distributed under the terms and conditions of the Creative Commons Attribution (CC BY) license (<https://creativecommons.org/licenses/by/4.0/>).

1. Introduction

Many applications in electrical engineering, medicine, outdoor weather control application, secure communication techniques, and so on are based by the study of chaotic dynamic systems. Therefore, many techniques have been developed to study the perturbation of this simple periodic motion.

Even if the one dimensional harmonic oscillator potential is a suitable model for a series of physical problems, in many cases the concordance with the experimental values is not sufficient. A typical example is the diatomic molecule whose motions, especially vibrations, cannot be described sufficiently by using the one dimensional harmonic oscillator potential. Among many models of anharmonic potentials a privileged position for the potential energy of a diatomic molecule is occupied by the Morse oscillator potential due to its applications in quantum mechanics [1] to diatomic or polyatomic molecules, spectroscopy, and so on. This is a convenient model because it explicitly includes the effects of bond breaking, as well as the existence of unbound states, the anharmonicity of real bonds and bond dissociation. A modified version of anharmonic potential is used in different applications in nonlinear dynamical systems to solve the inverse scattering problem to derive so called soliton solutions [2].

Recently, He et al. [3] adopted a generalized Duffing oscillator using the homotopy perturbation method (HPM). Bel et al. [4] analyzed the synchronization and stability of coupled driven-damped Helmholtz-Duffing oscillators in bi-stability regimes. Synchronization of a nonlinear oscillator was explored by Vieira et al. [5]. Mariano et al. [6] considered a general class of nonlinear dynamical systems with memory. Furthermore, nonlinear oscillators equipped with fast varying periodic time delay feedback were developed by

Liu et al. [7] using an analytical criterion. The mathematical techniques as periodic perturbations, stability, chaotic and asymptotic behaviors, and geometrical properties were developed in [8–19].

The Chen system [20] proposed in 1999, appears in a variety of studies, such as: Toda Lattice [21], Kowalevski top dynamics [22], Lotka–Volterra system [23], the battery model [24], Lagrange system [25], and others [26].

The relevance of the Chen chaotic system results from several approaches. For instance, an output feedback control algorithm for a single-input single-output variant was proposed in [27], the influence of the time delay was investigated in [28] showing that the single-scroll attractor is indeed chaotic, the global boundedness was explored in [29] using a suitable Lyapunov function, the equilibrium point stabilization problem by employing a simple linear feedback controller was discussed in [30], and others [31–39].

The aim of this work is to obtain the approximate closed-form solutions of the Chen system for a special case: just one analytic first integral known. For this case the Chen system could be reduced to an anharmonic oscillator which characterizes the behaviour of more physical systems of interest.

This paper is organized as follows. We focus on the analytical approaches of the approximate closed-form solutions for a special case of the Chen chaotic system in Section 2. In Section 3 we firstly proposed the differential equation which describes the nonlinear anharmonic oscillator. The OHAM method developed in [40–42] is applied for obtaining an approximate analytic solutions. Here, the study of the Chen chaotic system is reduced to a nonlinear anharmonic oscillator. Section 4 is devoted to the numerical simulations. There is an excellent agreement between the analytic approximate solution and the corresponding numerical solution which proved the validity of all obtained results. The last Section 5 is dedicated to some concluding remarks.

2. Approximate Closed-Form Solutions to the Chen’s System

The Chen system was analytically solved by mathematical techniques as the multistage homotopy–perturbation method in [33], the multistage homotopy analysis method [34], the differential transformation method (DTM) [36], the Adomian decomposition method (ADM), [37], the mechanical analysis [43], and the geometrical frame [44].

The Chen’s system has the form:

$$\begin{cases} \dot{x} = a(y - x) \\ \dot{y} = (c - a)x - xz + cy \\ \dot{z} = -bz + xy \end{cases} \quad (1)$$

where a, b, c are real parameters. The system is chaotic when $a = 35, b = 3, c = 28$ ([45]).

Remark 1. (a) If $a = 0$ and $b = c$ the system (1) has the Hamilton–Poisson realization. The functional $H(x, y, z) = x$ is the Hamiltonian and the $C(x, y, z) = \frac{1}{2}(-2cxz + 2yz + xy^2 + xz^2)$ is functionally independent Casimir. Thus, the exact solution is written as an intersection between the surfaces $H = cst$ and $C = cst$.

(b) For $a \in \mathbb{R}^*, b = c = 0$, the Hamiltonian function is $H(x, y, z) = y^2 + z^2 + 2az$, but finding the Casimir functions remains an open problem. Therefore, it is impossible to write the exact solution as an intersection between the surfaces $H = cst$ and $C = cst$.

(c) Otherwise, the Chen’s system is chaotic.

In the following we focus just on the case $a \in \mathbb{R}^*, b = c = 0$.

The system (1) becomes:

$$\begin{cases} \dot{x} = a(y - x) \\ \dot{y} = -ax - xz \\ \dot{z} = xy \end{cases} \quad (2)$$

Remark 2. The considered system admits a symmetry with respect to Oz- axis, for $a \in \mathbb{R}^*$, $b = c = 0$.

Considering the following representation:

$$\begin{cases} y = R \cdot \frac{2 \cdot w}{1+w^2} \\ z = -a + R \cdot \frac{1-w^2}{1+w^2} \end{cases}, \tag{3}$$

for the system (2) with $R^2 = [y(0)]^2 + (z(0) + a)^2$, Equation (2₃) gives

$$x = -\frac{2 \cdot \dot{w}}{1+w^2}. \tag{4}$$

Equation (2₂) identically satisfies, and Equation (2₁) yields:

$$\ddot{w}(t) + a \cdot \dot{w}(t) + a \cdot R \cdot w(t) = 2 \cdot \frac{w(t)}{1+w^2(t)} \cdot (\dot{w}(t))^2, \quad t > 0, \tag{5}$$

which describes the a nonlinear anharmonic oscillator presented in details in the following section.

For the unknown function w the initial conditions are:

$$w(0) = \frac{y(0)}{R+z(0)+a}, \quad \dot{w}(0) = -\frac{x(0)}{2} \cdot (1+w(0)^2). \tag{6}$$

For the nonlinear differential problem (5) and (6), the first-order approximate solutions, taking account of the following section and Equations (3) and (4), become:

$$\begin{cases} \bar{x} = -\frac{2 \cdot \dot{\bar{w}}}{1+\bar{w}^2} \\ \bar{y} = R \cdot \frac{2 \cdot \bar{w}}{1+\bar{w}^2} \\ \bar{z} = -a + R \cdot \frac{1-\bar{w}^2}{1+\bar{w}^2} \end{cases}. \tag{7}$$

3. Application to the Nonlinear Anharmonic Oscillator

The nonlinear anharmonic oscillator given by Equation (5) in our approach could be described by the following equation:

$$\ddot{w}(t)(1+w^2(t)) + a \cdot \dot{w}(t)(1+w^2(t)) + a \cdot R \cdot w(t)(1+w^2(t)) - 2 \cdot w(t) \cdot (\dot{w}(t))^2 = 0, \quad t > 0, \tag{8}$$

subject to the initial conditions:

$$w(0) = A_1, \quad \dot{w}(0) = B_1, \tag{9}$$

with $A_1 = \frac{y(0)}{R+z(0)+a} \neq 0$, $B_1 = -\frac{x(0)}{2} \cdot (1+w(0)^2) \neq 0$, $R = \sqrt{[y(0)]^2 + (z(0) + a)^2}$, $a \in \mathbb{R}$ given real numbers.

Taking into account of the initial conditions given by Equation (9), the approximate solutions, denoted $\bar{w}(t)$, of Equation (8) are deducted for the unknown function $w(t)$.

By using OHAM method (Marinca and Herisanu [40–42], for more details) to Equations (8) and (9) an analytic approximate solution, denoted $\bar{w}_{OHAM}(t)$, is obtained using only one iteration.

For an embedding parameter $p \in [0, 1]$, the first-order approximate solution \bar{w} for nonlinear differential problem given by Equations (8) and (9) could be written as:

$$\bar{w}(t) = w_0(t) + p \cdot w_1(t, C_j), \tag{10}$$

with $w_0(t)$ the initial approximation and $w_1(t, C_j)$ the first approximation depending on the variable t and the several unknown optimal parameters $C_1, C_2, C_3, \dots, C_{N_{max}}$, with N_{max} an arbitrary integer number.

The homotopic relation is given by [41]:

$$\begin{aligned} \mathcal{H} \left[\mathcal{L} \left(\bar{w}(t) \right), H(t, C_i, p), \mathcal{N} \left(\bar{w}(t) \right) \right] &= \\ &= (1 - p) \cdot \mathcal{L} \left(\bar{w}(t) \right) - H(t, C_i, p) \cdot \left[\mathcal{L} \left(\bar{w}(t, C_i) \right) + \mathcal{N} \left(\bar{w}(t) \right) \right] = 0, \end{aligned} \tag{11}$$

where the nonlinear operator $\mathcal{N}(\bar{w}(t))$ has the form

$$\mathcal{N}(\bar{w}(t)) = N_0(w_0(t)) + \sum_{m \geq 1} N_m(w_0, w_1, \dots, w_m) \cdot p^m \tag{12}$$

and $H(t, C_i, p) = p h_1(t, C_i) + p^2 h_2(t, C_i) + p^3 h_3(t, C_i) + \dots$ is a known auxiliary function. Taking into account Equations (10) and (12) the homotopic relation from Equation (11) becomes:

$$\mathcal{H} \left[\mathcal{L} \left(\bar{w}(t) \right), H(t, C_i), \mathcal{N} \left(\bar{w}(t) \right) \right] = \mathcal{L} \left(w_0(t) \right) + p \left[\mathcal{L} \left(w_1(t, C_i) \right) - H(t, C_i) \mathcal{N} \left(w_0(t) \right) \right] = 0, \tag{13}$$

where $H(t, C_i) \neq 0$ is an auxiliary convergence-control function depending of the variable t and of the parameters $C_1, C_2, \dots, C_{N_{max}}$. The linear operator $\mathcal{L}(w)$ has the form:

$$\mathcal{L}(w)(t) = \ddot{w} + 2K \cdot \dot{w} + (K^2 - \omega_0^2)w, \tag{14}$$

where $K, \omega_0 > 0$ are unknown parameters at this moment.

Therefore, the form of the nonlinear operator $\mathcal{N}(w)$ corresponding to the unknown function w is obtained from Equation (8) by:

$$\begin{aligned} \mathcal{N}(w)(t) &= -2K \cdot \dot{w} - (K^2 - \omega_0^2)w + \ddot{w}(t) \cdot w^2(t) - 2 \cdot w(t) \cdot (\dot{w}(t))^2 + \\ &+ a \cdot \dot{w}(t) \cdot (1 + w^2(t)) + a \cdot R \cdot (1 + w^2(t)) \cdot w(t). \end{aligned} \tag{15}$$

The deformations problems are obtained by identifying the coefficients p^0 and p^1 , respectively.

Some possibilities to choose the auxiliary function $H(t, C_i)$ could be:

$$H(t, C_i) = \sum_{k=1}^{N_{max}} a_k^{(2)} \cdot \cos(2k + 1)\omega_0 t + b_k^{(2)} \cdot \sin(2k + 1)\omega_0 t, \tag{16}$$

where $C_i \in \{a_k^{(2)} \mid k = \overline{1, N_{max}}\} \cup \{b_k^{(2)} \mid k = \overline{1, N_{max}}\}$, or

$$H(t, C_i) = C_1 \cos(\omega_0 t) + B_1 \sin(\omega_0 t),$$

or

$$H(t, C_i) = C_1 \cos(\omega_0 t) + B_1 \sin(\omega_0 t) + C_2 \cos(3\omega_0 t) + B_2 \sin(3\omega_0 t),$$

or

$$H(t, C_i) = C_1 \cos(\omega_0 t) + B_1 \sin(\omega_0 t) + C_2 \cos(3\omega_0 t) + B_2 \sin(3\omega_0 t) + C_3 \cos(5\omega_0 t) + B_3 \sin(5\omega_0 t),$$

and so on.

3.1. The Zeroth-Order Deformation Problem

For the initial approximation w_0 , Equation (14) becomes:

$$\ddot{w} + 2K \cdot \dot{w} + (K^2 - \omega_0^2)w = 0, \quad w(0) = A_1, \quad \dot{w}(0) = B_1 \tag{17}$$

with the solution

$$w_0(t) = w(0) e^{-K t} \cos(\omega_0 t) + \frac{\dot{w}(0)}{\omega_0} e^{-K t} \sin(\omega_0 t). \tag{18}$$

3.2. The First-Order Deformation Problem

The nonlinear operator Equation (15) for the initial approximation $w_0(t)$ given by Equation (18), using Equation (15) becomes:

$$\mathcal{N}(w_0)(t) = M_1 \cdot e^{-K t} \cdot \cos(\omega_0 t) + M_2 \cdot e^{-3K t} \cdot \cos(\omega_0 t) + M_3 \cdot e^{-3K t} \cdot \cos(3\omega_0 t) + P_1 \cdot e^{-K t} \cdot \sin(\omega_0 t) + P_2 \cdot e^{-3K t} \cdot \sin(\omega_0 t) + P_3 \cdot e^{-3K t} \cdot \sin(3\omega_0 t), \tag{19}$$

where

$$\begin{aligned} M_1 &= aB_1 - aKA_1 - 2KB_1 + A_1K^2 + aRA_1 + A_1\omega_0^2, \\ M_2 &= \frac{1}{4}aA_1^2B_1 - \frac{5}{4}A_1B_1^2 - \frac{3}{4}aKA_1^3 + \frac{1}{2}KA_1^2B_1 - \frac{3}{4}K^2A_1^3 + \frac{3}{4}aRA_1^3 + \\ &+ \frac{aB_1^3}{4\omega_0^2} - \frac{3aKA_1B_1^2}{4\omega_0^2} + \frac{KB_1^3}{2\omega_0^2} - \frac{3K^2A_1B_1^2}{4\omega_0^2} + \frac{3aRA_1B_1^2}{4\omega_0^2} - \frac{5}{4}A_1^3\omega_0^2, \\ M_3 &= \frac{3}{4}aA_1^2B_1 - \frac{3}{4}A_1B_1^2 - \frac{1}{4}aKA_1^3 + \frac{3}{2}KA_1^2B_1 - \frac{1}{4}K^2A_1^3 + \frac{1}{4}aRA_1^3 - \\ &- \frac{aB_1^3}{4\omega_0^2} + \frac{3aKA_1B_1^2}{4\omega_0^2} - \frac{KB_1^3}{2\omega_0^2} + \frac{3K^2A_1B_1^2}{4\omega_0^2} - \frac{3aRA_1B_1^2}{4\omega_0^2} + \frac{1}{4}\omega_0^2A_1^3 \\ P_1 &= -\frac{aKB_1}{\omega_0} + \frac{K^2B_1}{\omega_0} + \frac{aRB_1}{\omega_0} - a\omega_0A_1 + B_1\omega_0 + 2K\omega_0A_1, \\ P_2 &= -\frac{3aKB_1^3}{4\omega_0^3} - \frac{3K^2B_1^3}{4\omega_0^3} + \frac{3aRB_1^3}{4\omega_0^3} - \frac{aA_1B_1^2}{4\omega_0} - \frac{5B_1^3}{4\omega_0} - \frac{3aKA_1^2B_1}{4\omega_0} - \frac{KA_1B_1^2}{2\omega_0} - \\ &- \frac{3K^2A_1^2B_1}{4\omega_0} + \frac{3aRA_1^2B_1}{4\omega_0} - \frac{1}{4}a\omega_0A_1^3 - \frac{5}{4}\omega_0A_1^2B_1 - \frac{1}{2}K\omega_0A_1^3 \\ P_3 &= \frac{aKB_1^3}{4\omega_0^3} + \frac{K^2B_1^3}{4\omega_0^3} - \frac{aRB_1^3}{4\omega_0^3} + \frac{3aA_1B_1^2}{4\omega_0} - \frac{B_1^3}{4\omega_0} - \frac{3aKA_1^2B_1}{4\omega_0} + \frac{3KA_1B_1^2}{2\omega_0} - \\ &- \frac{3K^2A_1^2B_1}{4\omega_0} + \frac{3aRA_1^2B_1}{4\omega_0} - \frac{1}{4}a\omega_0A_1^3 + \frac{3}{4}\omega_0A_1^2B_1 - \frac{1}{2}KA_1^3 \end{aligned}$$

It depends on the elementary functions $e^{-K t} \cdot \cos(\omega_0 t)$, $e^{-3K t} \cdot \cos(\omega_0 t)$, $e^{-3K t} \cdot \cos(3\omega_0 t)$, $e^{-K t} \cdot \sin(\omega_0 t)$, $e^{-3K t} \cdot \sin(\omega_0 t)$, $e^{-3K t} \cdot \sin(3\omega_0 t)$. For $p = 1$, from Equation (13) the first-order deformation problem becomes:

$$\mathcal{L}(w_1(t, C_i)) = H(t, C_i)\mathcal{N}(w_0(t)) \tag{20}$$

By integration of the first approximation $w_1(t, C_i)$, from Equation (20) and considering for $H(t, C_i)$ the expression given by Equation (16) yields:

$$w_1(t, C_i) = \sum_{k=1}^{N_{max}} C_k \cdot e^{-3K t} \cdot \cos((2k + 1)\omega_0 t) + B_k \cdot e^{-3K t} \cdot \sin((2k + 1)\omega_0 t), \tag{21}$$

where C_i , B_i are unknown parameters, with $\sum_{k=1}^{N_{max}} C_k = 0$ and $\sum_{k=1}^{N_{max}} (2k + 1) \cdot B_k = 0$, respectively.

3.3. The First-Order Analytical Approximate Solution \bar{w}

Taking into account of Equations (18) and (21) was obtained the first-order approximate solution given by Equation (10), when $p = 1$ in the form:

$$\bar{w}(t) = w_0(t) + w_1(t, C_i) = w(0) e^{-K t} \cos(\omega_0 t) + \frac{\dot{w}(0)}{\omega_0} e^{-K t} \sin(\omega_0 t) + \sum_{k=1}^{N_{max}} C_k \cdot e^{-3K t} \cdot \cos((2k + 1)\omega_0 t) + B_k \cdot e^{-3K t} \cdot \sin((2k + 1)\omega_0 t), \tag{22}$$

where the unknown parameters $C_i, B_i, i = 1, 2, 3, \dots$, are optimally identified.

4. Numerical Simulation

In order to demonstrate the accuracy and validity of the OHAM technique, a comparison between our approximate solutions with corresponding numerical results obtained via the fourth-order Runge–Kutta method is highlighted.

We consider the initial value problem given by (2) with initial conditions $x(0) = 1, y(0) = 1, z(0) = 1, a = 0.25$ and $b = c = 0$. The convergence-control parameters $K, \omega_0, \{B_i\}_{i=1, N_{max}}, \{C_i\}_{i=1, N_{max}}$ are optimally determined by means of the least-square method.

Tables 1–4 emphasizes the accuracy of the OHAM technique by comparing the approximate analytic solutions $\bar{w}, \bar{x}, \bar{y}$, and \bar{z} , presented above with the corresponding numerical integration values (via the fourth-order Runge–Kutta method). These comparisons show the effectiveness, reliability, applicability, and efficiency of the OHAM.

Table 1. Comparison between the analytical approximate solution \bar{w}_{OHAM} of Equation (22) and the corresponding numerical values for different values of the index number N_{max} .

t	$N_{max} = 10$	$N_{max} = 15$	$N_{max} = 20$	$N_{max} = 25$
	$w_{numerical}$			
0		0.35078105		
1.7		−0.40330489		
3.4		−0.63904518		
5.1		−0.29126219		
6.8		0.12552955		
8.5		0.29643558		
10.2		0.16028326		
11.9		−0.05820289		
13.6		−0.15188552		
15.3		−0.08407041		
17		0.03107464		
	\bar{w}_{OHAM} obtained from Equation (22) and			
	Equation (A1)	Equation (A2)	Equation (A3)	Equation (A4)
0	0.35078105	0.35078105	0.35078105	0.35078105
1.7	−0.40841782	−0.40330994	−0.40330493	−0.40330493
3.4	−0.64462314	−0.63904979	−0.63904521	−0.63904521
5.1	−0.29646094	−0.29126751	−0.29126222	−0.29126223
6.8	0.12060783	0.12552535	0.12552950	0.12552951
8.5	0.28751514	0.29643084	0.29643554	0.29643554
10.2	0.14938850	0.16027866	0.16028322	0.16028322
11.9	−0.06828322	−0.05819707	−0.05820297	−0.05820293
13.6	−0.16709523	−0.15188883	−0.15188558	−0.15188556
15.3	−0.09821857	−0.08408416	−0.08407045	−0.08407044
17	0.01573297	0.03106425	0.03107455	0.03107461

Table 1. Cont.

t	$N_{max} = 10$	$N_{max} = 15$	$N_{max} = 20$	$N_{max} = 25$
Relative errors = $ w_{numerical} - \bar{w}_{OHAM} $				
0	5.689×10^{-14}	5.551×10^{-17}	5.689×10^{-14}	2.841×10^{-13}
1.7	0.00511292	5.049×10^{-6}	3.829×10^{-8}	3.423×10^{-8}
3.4	0.00557796	4.616×10^{-6}	3.491×10^{-8}	3.438×10^{-8}
5.1	0.00519875	5.321×10^{-6}	3.786×10^{-8}	4.167×10^{-8}
6.8	0.00492171	4.197×10^{-6}	4.579×10^{-8}	4.043×10^{-8}
8.5	0.00892043	4.732×10^{-6}	3.524×10^{-8}	3.975×10^{-8}
10.2	0.01089475	4.599×10^{-6}	3.694×10^{-8}	4.065×10^{-8}
11.9	0.01008032	5.821×10^{-6}	7.353×10^{-8}	3.995×10^{-8}
13.6	0.01520970	3.307×10^{-6}	5.836×10^{-8}	3.493×10^{-8}
15.3	0.01414815	1.374×10^{-5}	3.568×10^{-8}	2.826×10^{-8}
17	0.01534166	1.039×10^{-5}	8.433×10^{-8}	3.114×10^{-8}

Table 2. Comparison between the analytic closed-form approximate solution \bar{x} given by Equation (7)₁ and corresponding numerical solution; the relative errors $\epsilon_x = |x_{numerical} - \bar{x}_{OHAM}|$.

t	$x_{numerical}$	\bar{x}_{OHAM}	Relative Errors ϵ_x
0	1	0.99999998	1.781×10^{-8}
1.7	0.57062883	0.57062880	3.337×10^{-8}
3.4	−0.10808510	−0.1080850	4.599×10^{-8}
5.1	−0.49392956	−0.4939297	1.456×10^{-7}
6.8	−0.38333158	−0.3833315	8.265×10^{-8}
8.5	0.00446477	0.0044648	3.685×10^{-8}
10.2	0.25485018	0.2548503	1.881×10^{-7}
11.9	0.20964292	0.2096428	2.959×10^{-8}
13.6	0.00265313	0.0026531	2.432×10^{-8}
15.3	−0.13494391	−0.1349440	9.170×10^{-8}
17	−0.11083968	−0.1108396	2.099×10^{-8}

Table 3. Comparison between the analytic closed-form approximate solution \bar{y} given by Equation (7)₂ and corresponding numerical solution; the relative errors $\epsilon_y = |y_{numerical} - \bar{y}_{OHAM}|$.

t	$y_{numerical}$	\bar{y}_{OHAM}	Relative Errors ϵ_y
0	1	1.0000000000006326	6.326×10^{-13}
1.7	−1.11056659	−1.11056670	1.180×10^{-7}
3.4	−1.45269382	−1.45269367	1.479×10^{-7}
5.1	−0.85957282	−0.85957335	5.275×10^{-7}
6.8	0.39565568	0.39565592	2.411×10^{-7}
8.5	0.87239595	0.87239585	9.511×10^{-8}
10.2	0.50030350	0.50030353	3.028×10^{-8}
11.9	−0.18571072	−0.18571121	4.917×10^{-7}
13.6	−0.47530599	−0.47530611	1.210×10^{-7}
15.3	−0.26726775	−0.26726775	8.200×10^{-9}
17	0.09939116	0.09939132	1.591×10^{-7}

Table 4. Comparison between the analytic closed-form approximate solution \bar{z} given by Equation (7)₃ and corresponding numerical solution; the relative errors $\epsilon_z = |z_{numerical} - \bar{z}_{OHAM}|$.

t	$z_{numerical}$	\bar{z}_{OHAM}	Relative Errors ϵ_z
0	1	0.999999999999494	5.060×10^{-13}
1.7	0.90288415	0.90288402	1.293×10^{-7}
3.4	0.42244420	0.42244411	8.863×10^{-8}
5.1	1.10041934	1.10041980	4.580×10^{-7}
6.8	1.30111457	1.30111456	1.648×10^{-8}
8.5	1.09217208	1.09217192	1.641×10^{-7}
10.2	1.27059023	1.27059079	5.585×10^{-7}
11.9	1.33997205	1.33997212	6.118×10^{-8}
13.6	1.27858895	1.27858892	3.430×10^{-8}
15.3	1.32831159	1.32831174	1.498×10^{-7}
17	1.34769247	1.34769251	3.643×10^{-8}

All the convergence-control parameters, corresponding to the intervals $[0, 20]$ are presented in Appendix A.

Figures 1–3 present the comparisons between the analytical approximate solutions given by OHAM and numerical results provided by Runge–Kutta fourth steps integrator, for initial conditions $x(0) = 1, y(0) = 1, z(0) = 1, a = 0.25$ and for $N_{max} = 25$. From these figures it follows that the behavior of the analytical approximate solutions and Runge–Kutta fourth steps integrator’s results are quite the same.

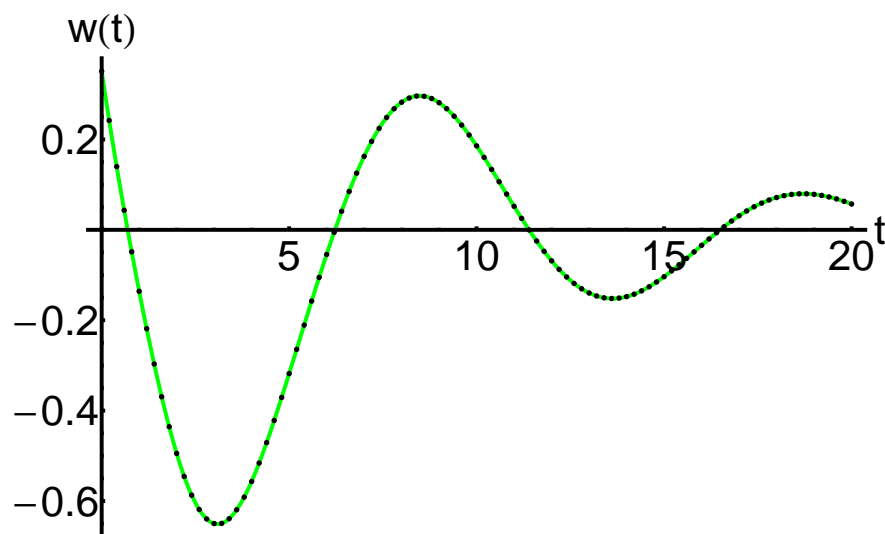


Figure 1. Comparison between the analytical approximate solution \bar{w}_{OHAM} of Equation (22) and the corresponding numerical solution: numerical solution (with lines) and OHAM solution (dashing lines), respectively.

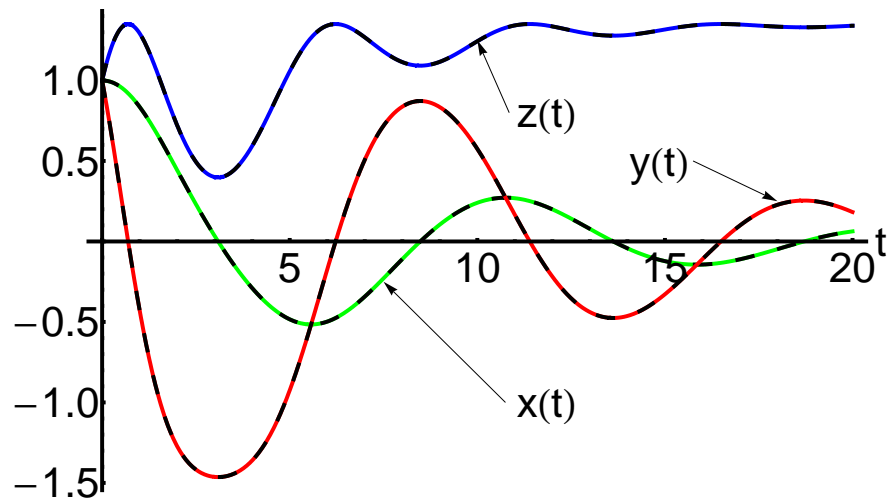


Figure 2. Comparison between the approximate closed-form solutions $\bar{x}(t)$, $\bar{y}(t)$, $\bar{z}(t)$ of the Chen system given by Equation (7) and corresponding numerical solution: numerical solution (with lines) and OHAM solution (dashing lines), respectively.

The corresponding relative errors are presented in detail in Appendix A.

Below we highlight the advantages of the OHAM method by comparison with an iterative method developed in [46]. By integration of the system (2) over the interval $[0, t]$, the following relations are obtained:

$$\begin{aligned} x(t) &= x(0) + \int_0^t a(y(s) - x(s)) ds \\ y(t) &= y(0) + \int_0^t (-ax(s) - x(s)z(s)) ds \quad . \\ z(t) &= z(0) + \int_0^t x(s)y(s) ds \end{aligned} \tag{23}$$

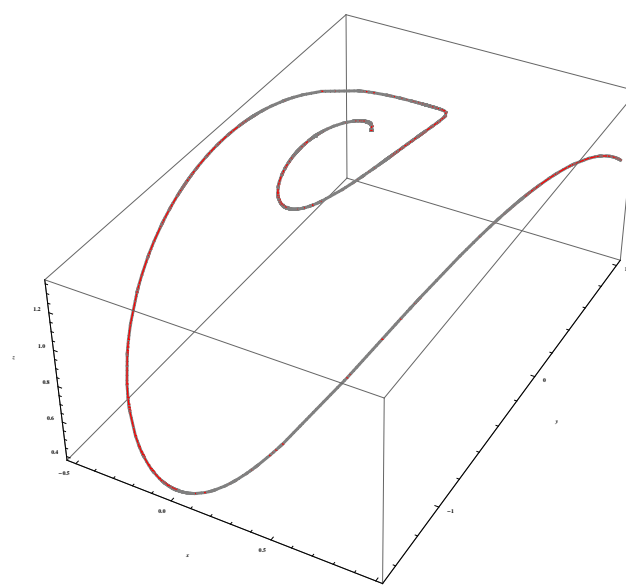


Figure 3. The parametric curve $(\bar{x}(t), \bar{y}(t), \bar{z}(t))$ is the 3D-trajectory of the Chen system: numerical solution (with lines) and OHAM solution (dashing lines), respectively.

The iterative algorithm is the following:

$$\begin{aligned}
 x_0(t) &= x(0), & x_1(t) &= N_1(x_0, y_0, z_0) = \int_0^t a(y_0(s) - x_0(s)) ds, \\
 y_0(t) &= y(0), & y_1(t) &= N_2(x_0, y_0, z_0) = \int_0^t (-ax_0(s) - x_0(s)z_0(s)) ds, \\
 z_0(t) &= z(0), & z_1(t) &= N_3(x_0, y_0, z_0) = \int_0^t x_0(s)y_0(s) ds,
 \end{aligned} \tag{24}$$

$$\begin{aligned}
 x_m(t) &= N_1(x_0 + x_1 + \dots + x_{m-1}, y_0 + y_1 + \dots + y_{m-1}, z_0 + z_1 + \dots + z_{m-1}) - \\
 &\quad - N_1(x_0 + x_1 + \dots + x_{m-2}, y_0 + y_1 + \dots + y_{m-2}, z_0 + z_1 + \dots + z_{m-2}), \\
 y_m(t) &= N_2(x_0 + x_1 + \dots + x_{m-1}, y_0 + y_1 + \dots + y_{m-1}, z_0 + z_1 + \dots + z_{m-1}) - \\
 &\quad - N_2(x_0 + x_1 + \dots + x_{m-2}, y_0 + y_1 + \dots + y_{m-2}, z_0 + z_1 + \dots + z_{m-2}), \\
 z_m(t) &= N_3(x_0 + x_1 + \dots + x_{m-1}, y_0 + y_1 + \dots + y_{m-1}, z_0 + z_1 + \dots + z_{m-1}) - \\
 &\quad - N_3(x_0 + x_1 + \dots + x_{m-2}, y_0 + y_1 + \dots + y_{m-2}, z_0 + z_1 + \dots + z_{m-2}), \quad m \geq 2.
 \end{aligned}$$

With the iterative method, the solutions of system (2) have the form:

$$x_{iter}(t) = \sum_{m=0}^{\infty} x_m(t), \quad y_{iter}(t) = \sum_{m=0}^{\infty} y_m(t), \quad z_{iter}(t) = \sum_{m=0}^{\infty} z_m(t).$$

For the case using seven iterations, with the initial conditions $x(0) = 1, y(0) = 1, z(0) = 1$ and the constants $a = 0.25, b = c = 0$, taking into account of the algorithm (24), the iterative solutions become:

$$\begin{aligned}
 x_{iter}(t) &= \sum_{m=0}^7 x_m(t) = 1 - 0.15625t^2 - 0.02864583t^3 + 0.01888020t^4 + 0.00419108t^5 - \\
 &\quad - 0.00186326t^6 - 0.00066741t^7 + 0.00016160t^8 + 0.00008497t^9 - 9.153078 \cdot 10^{-6}t^{10} - \\
 &\quad - 8.689161 \cdot 10^{-6}t^{11} + 6.523628 \cdot 10^{-8}t^{12} + 7.013146 \cdot 10^{-7}t^{13} + 5.223197 \cdot 10^{-8}t^{14} - 4.322356 \cdot 10^{-8}t^{15}, \\
 y_{iter}(t) &= \sum_{m=0}^7 y_m(t) = 1 - 1.25t - 0.5t^2 + 0.2734375t^3 + 0.10270182t^4 - 0.04052734t^5 - \\
 &\quad - 0.0205508t^6 + 0.00508378t^7 + 0.0034984t^8 - 0.00048158t^9 - 0.0005136t^{10} + 0.00002626t^{11} + \\
 &\quad + 0.0000650t^{12} + 1.353350 \cdot 10^{-6}t^{13} - 7.134374 \cdot 10^{-6}t^{14} - 6.095126 \cdot 10^{-7}t^{15} + 6.773822 \cdot 10^{-7}t^{16} + \\
 &\quad + 1.007179 \cdot 10^{-7}t^{17} - 5.542185 \cdot 10^{-8}t^{18} - 1.201667 \cdot 10^{-8}t^{19}, \\
 z_{iter}(t) &= \sum_{m=0}^7 z_m(t) = 1 + t - 0.625t^2 - 0.21874999t^3 + 0.11002604t^4 + 0.04710286t^5 - \\
 &\quad - 0.01472303t^6 - 0.00871044t^7 + 0.00159948t^8 + 0.00138481t^9 - 0.00011177t^{10} - 0.00018913t^{11} - \\
 &\quad - 7.689201 \cdot 10^{-7}t^{12} + 0.00002208t^{13} + 1.751434 \cdot 10^{-6}t^{14} - 2.202022 \cdot 10^{-6}t^{15} - 3.375254 \cdot 10^{-7}t^{16} + \\
 &\quad + 1.858551 \cdot 10^{-7}t^{17} + 4.383605 \cdot 10^{-8}t^{18} - 1.298323 \cdot 10^{-8}t^{19} - 4.480401 \cdot 10^{-9}t^{20}.
 \end{aligned} \tag{25}$$

A comparison between approximate closed-form solutions $\bar{x}_{OHAM}, \bar{y}_{OHAM}, \bar{z}_{OHAM}$ and the corresponding iterative solutions $x_{iter}, y_{iter}, z_{iter}$ given in (25) is shown in the Appendix A both graphically in Figure 4 and tabularly in Table 5, respectively.

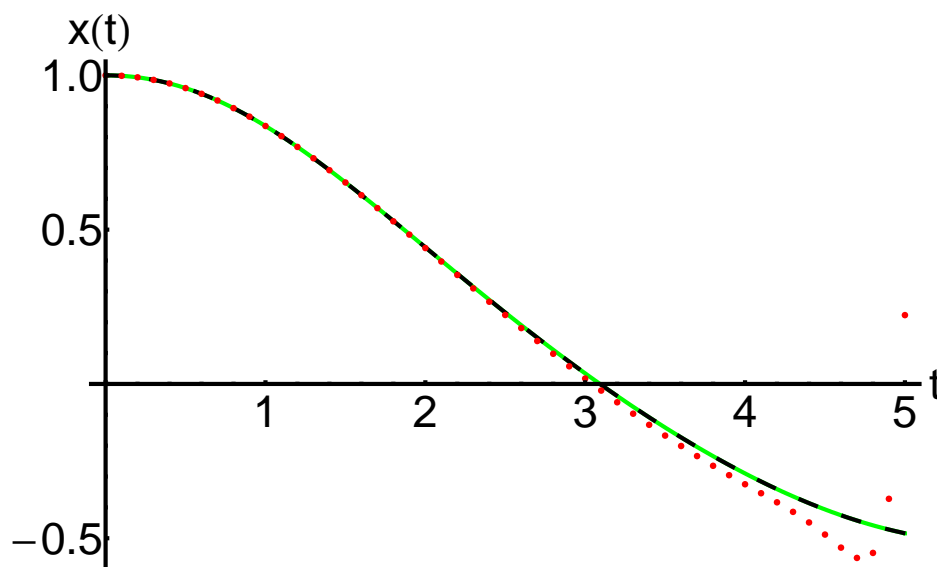


Figure 4. Comparison between the approximate closed-form solution $\bar{x}(t)$, of the Chen system given by Equation (7), corresponding numerical solution and the iterative solution $x_{iter}(t)$ given by Equation (25): numerical solution (with lines), OHAM solution (dashing lines), and iterative solution (dotted curve), respectively.

This comparison shows the precision and efficiency of the OHAM method (using just one iteration) against to the iterative method described in [46] (using seven iterations).

Table 5. Comparison between the approximate closed-form solution \bar{x} given by Equation (7)₁, corresponding numerical solution and the iterative solution x_{iter} given by Equation (25).

t	$x_{numerical}$	\bar{x}_{OHAM}	x_{iter}
0	1	0.99999998	1
1/2	0.95863428	0.95863428	0.95863421
1	0.83589390	0.83589396	0.83587428
3/2	0.65318706	0.65318710	0.65280614
2	0.44281996	0.44281983	0.44040998
5/2	0.23134451	0.23134437	0.22345920
3	0.03418218	0.03418216	0.01748463
7/2	-0.14118335	-0.14118327	-0.16734859
4	-0.28999110	-0.28999104	-0.32509324
9/2	-0.40661666	-0.40661673	-0.48802039
5	-0.48384683	-0.48384691	0.22295502

5. Conclusions

For a special case of the Chen system (just one analytic first integral) is shown that this system could be reduced to a nonlinear anharmonic oscillator. An analytic approximate solution for the anharmonic oscillator problem was been obtained by means of the Optimal Homotopy Asymptotic Method. The numerical outcomes contribute to a better knowledge of the accuracy and validity of the OHAM technique. The flexibility of this method results from the comparison with the corresponding iterative procedure. The results of our present study are useful in understanding of the behavior for the dynamical systems as complete synchronization or optimization of nonlinear system performance.

Author Contributions: Conceptualization, N.P.; Data curation, R.-D.E. and N.P.; Formal analysis, N.P.; Investigation, R.-D.E. and N.P.; Methodology, R.-D.E.; Software, R.-D.E.; Supervision, N.P.; Validation, R.-D.E. and N.P.; Visualization, R.-D.E. and N.P.; Writing—original draft, R.-D.E. and N.P. All authors have read and agreed to the published version of the manuscript.

Funding: This research received no external funding.

Institutional Review Board Statement: Not applicable.

Informed Consent Statement: Not applicable.

Data Availability Statement: Not applicable.

Conflicts of Interest: The authors declare no conflict of interest.

Appendix A

In the following we will present just the values of the convergence-control parameters that appear in Equation (22); for $a = 0.25$, the initial conditions are $x_0 = 1, y_0 = 1, z_0 = 1$, and different values of the index number N_{max} .

Example A1. $N_{max} = 10$:

$$\begin{aligned} K &= 0.125, \omega_0 = 0.09341358, B_1 = -474.05746504, B_2 = -83.66952872, \\ B_3 &= 983.93349991, B_4 = 93.11707785, B_5 = -613.37703852, \\ B_6 &= -92.46381246, B_7 = 185.13599744, B_8 = 22.90934052, \\ B_9 &= -21.15973503, B_{10} = -0.36833594, C_1 = -105.19741270, \\ C_2 &= 864.84740763, C_3 = 73.00030471, C_4 = -852.78114752, \\ C_5 &= -110.08737855, C_6 = 370.62105410, C_7 = 55.55687516, \\ C_8 &= -73.53898242, C_9 = -5.45522779, C_{10} = 3.29519765; \end{aligned} \quad (A1)$$

Example A2. $N_{max} = 15$:

$$\begin{aligned} K &= 0.125, \omega_0 = 0.09341358, B_1 = -535.73029486, B_2 = -225.66684894, \\ B_3 &= 1247.98395161, B_4 = 448.29476171, B_5 = -949.41747655, \\ B_6 &= -520.95990410, B_7 = 388.66581563, B_8 = 298.76728809, \\ B_9 &= -79.92299107, B_{10} = -90.33265095, B_{11} = 5.37514330, \\ B_{12} &= 13.37723677, B_{13} = 0.27233992, B_{14} = -0.69635773, \\ B_{15} &= -0.01001282, C_1 = -158.38311092, C_2 = 1027.07825300, \\ C_3 &= 324.06915822, C_4 = -1182.48969116, C_5 = -532.36755526, \\ C_6 &= 656.26210797, C_7 = 427.80899081, C_8 = -194.45446761, \\ C_9 &= -178.15216326, C_{10} = 25.41293181, C_{11} = 38.43418910, \\ C_{12} &= -0.27099978, C_{13} = -3.63274094, C_{14} = -0.09466754, \\ C_{15} &= 0.07144867; \end{aligned} \quad (A2)$$

Example A3. $N_{max} = 20$:

$$\begin{aligned} K &= 0.125, \omega_0 = 0.09341358, B_1 = -572.08992817, B_2 = -363.49072823, \\ B_3 &= 1381.88608368, B_4 = 835.02442901, B_5 = -1066.96252972, \\ B_6 &= -1047.38729501, B_7 = 366.92483166, B_8 = 718.19317811, \\ B_9 &= 34.69590962, B_{10} = -288.65895012, B_{11} = -85.27528612, \\ B_{12} &= 65.37007538, B_{13} = 34.29919136, B_{14} = -6.61520810, \\ B_{15} &= -6.39869616, B_{16} = -0.08142131, B_{17} = 0.53154862, \\ B_{18} &= 0.04883938, B_{19} = -0.01315662, B_{20} = -0.00088725, \\ C_1 &= -204.77267749, C_2 = 1116.51695688, C_3 = 584.18123914, \\ C_4 &= -1329.27601259, C_5 = -1017.12141826, C_6 = 710.13206838, \\ C_7 &= 928.81089412, C_8 = -110.98469772, C_9 = -486.67750378, \\ C_{10} &= -88.11599375, C_{11} = 148.66520536, C_{12} = 60.17614458, \\ C_{13} &= -23.74134196, C_{14} = -16.23938481, C_{15} = 1.10909390, \\ C_{16} &= 2.06863981, C_{17} = 0.13314723, C_{18} = -0.10234454, \\ C_{19} &= -0.00970849, C_{20} = 0.00085215; \end{aligned} \quad (A3)$$

Example A4. $N_{max} = 25$:

$$\begin{aligned}
K &= 0.125, \omega_0 = 0.09341358, B_1 = -843.44077781, B_2 = -2283.08793538, \\
B_3 &= 963.47493402, B_4 = 5265.50493093, B_5 = 2381.34084725, \\
B_6 &= -4904.15706502, B_7 = -5195.34441243, B_8 = 1560.49523602, \\
B_9 &= 4556.65455444, B_{10} = 945.30628765, B_{11} = -2149.41196346, \\
B_{12} &= -1226.18931187, B_{13} = 489.36452965, B_{14} = 588.62871016, \\
B_{15} &= 11.77859750, B_{16} = -151.42839682, B_{17} = -36.81760967, \\
B_{18} &= 20.19657690, B_{19} = 9.01179313, B_{20} = -0.96835111, \\
B_{21} &= -0.91332857, B_{22} = -0.03411510, B_{23} = 0.03395935, \\
B_{24} &= 0.00251461, B_{25} = -0.00020438, C_1 = -854.03834610, \\
C_2 &= 1379.75774496, C_3 = 3964.31358727, C_4 = 452.62887014, \\
C_5 &= -5635.41300047, C_6 = -4149.93476429, C_7 = 3363.41705866, \\
C_8 &= 5285.44980443, C_9 = -22.27424250, C_{10} = -3377.83070642, \\
C_{11} &= -1308.19072093, C_{12} = 1150.99851855, C_{13} = 924.29822101, \\
C_{14} &= -133.76608326, C_{15} = -321.94225580, C_{16} = -45.68283663, \\
C_{17} &= 60.64935784, C_{18} = 20.54843020, C_{19} = -5.31528345, \\
C_{20} &= -3.19668710, C_{21} = 0.05591426, C_{22} = 0.20456572, \\
C_{23} &= 0.01371534, C_{24} = -0.00373301, C_{25} = -0.00020577.
\end{aligned} \tag{A4}$$

Now, for the initial conditions $x_0 = -1, y_0 = -1, z_0 = 1$, and $N_{max} = 25$, the convergence-control parameters for the symmetric solution (with respect to the Oz -axis) given by Equation (22) are given in Equation (A4).

References

1. Popov, D.; Dong, S.; Pop, N.; Sajfert, V.; Simon, S. Construction of the Barut–Girardello quasi coherent states for the Morse potential. *Ann. Phys.* **2013**, *339*, 122–134. [\[CrossRef\]](#)
2. Gupta, V.P. *Principles and Applications of Quantum Chemistry*; Academic Press: Cambridge, MA, USA, 2016; pp. 1–46.
3. He, J.; Jiao, M.; Gepreel, K.A.; Khan, Y. Homotopy perturbation method for strongly nonlinear oscillators. *Math. Comput. Simul.* **2023**, *204*, 243–258. [\[CrossRef\]](#)
4. Bel, G.; Alexandrov, B.S.; Bishop, A.R.; Rasmussen, K. Patterns and stability of coupled multi-stable nonlinear oscillators. *Chaos Solitons Fractals Interdiscip.* **2023**, *166*, 112999. [\[CrossRef\]](#) [\[PubMed\]](#)
5. Vieira, R.; Martins, W.S.; Barreiro, S.; de Oliveira, R.A.; Chevrollier, M.; Oria, M. Synchronization of a nonlinear oscillator with a sum signal from equivalent oscillators. *Chaos Solitons Fractals* **2021**, *153*, 111581. [\[CrossRef\]](#)
6. Mariano, P.M.; Spadini, M. Periodic solutions to perturbed nonlinear oscillators with memory. *Physica D* **2023**, *445*, 133635. [\[CrossRef\]](#)
7. Liu, Q.X.; Liu, J.K.; Chen, Y.M. An analytical criterion for alternate stability switches in nonlinear oscillators with varying time delay. *Int. J.-Non-Linear Mech.* **2020**, *126*, 103563. [\[CrossRef\]](#)
8. Bibikov, Y.N.; Savel'eva, A.G. Periodic Perturbations of a Nonlinear Oscillator. *Differ. Equ.* **2016**, *52*, 405–412. [\[CrossRef\]](#)
9. Kaparulin, D.S.; Lyakhovich, S.L. On the stability of a nonlinear oscillator with higher derivatives. *Russ. Phys. J.* **2015**, *57*, 1561–1565. [\[CrossRef\]](#)
10. Pei, Q.-Y.; Li, L. Chaotic behavior of a nonlinear oscillator. *Appl. Math. Mech.* **1993**, *14*, 395–405. [\[CrossRef\]](#)
11. Ginoux, J.M.; Rossetto, B. Differential geometry and mechanics: Applications to chaotic dynamical systems. *Int. J. Bifurcat. Chaos* **2006**, *16*, 887. [\[CrossRef\]](#)
12. Hernández-Bermejo, B.; Fairen, V. Simple evaluation of Casimirs invariants in finite dimensional Poisson systems. *Phys. Lett. A* **1998**, *241*, 148–154. [\[CrossRef\]](#)
13. Kahan, W. Unconventional numerical methods for trajectory calculation. *Unpubl. Lect. Notes* **1993**, *1*, 13.
14. Pop, C.; Petrisor, C.; Bala, D. Hamilton-Poisson Realizations for the Lü System. *Math. Probl. Eng.* **2011**, *2011*, 842325. [\[CrossRef\]](#)
15. Ariesanu, C.P. Numerical integration and Stability Problems in the Study of Lorenz System. *Acta Tech. Napoc.* **2011**, *54*, 333–339.
16. Puta, M. *Hamiltonian Systems and Geometric Quantization. Mathematics and Its Applications*; Springer: Berlin/Heidelberg, Germany, 1993; Volume 260.
17. Tudoran, R.M.; Aron, A.; Nicoara, S. On a Hamiltonian Version of the Rikitake System. *SIAM J. Appl. Dyn. Syst.* **2010**, *8*, 454–479. [\[CrossRef\]](#)
18. Anakira, N.R.; Alomari, A.K.; Jameel, A.; Hashim, I. Multistage optimal homotopy asymptotic method for solving initial-value problems. *J. Nonlinear Sci. App.* **2016**, *9*, 1826–1843. [\[CrossRef\]](#)
19. Khatibzadeh, H. Asymptotic Behavior of a Discrete Nonlinear Oscillator with Damping Dynamical System. *Adv. Differ. Equ.* **2011**, *2011*, 867136. [\[CrossRef\]](#)

20. Chen, G.; Ueta, T. Yet another chaotic attractor. *Int. J. Bifurcat. Chaos* **1999**, *9*, 1465–1466. [[CrossRef](#)]
21. Daminou, P.A. Multiple Hamiltonian structures for Toda systems of type A-B-C. *Regul. Chaotic Dyn.* **2000**, *5*, 17–32. [[CrossRef](#)]
22. Aron, A.; Puta, M. Stability, periodic solutions and numerical integration in the Kowalevski top dynamics. *Int. J. Geom. Methods M* **2006**, *3*, 1323–1330. [[CrossRef](#)]
23. Pop, C.; Aron, A.; Galea, C.; Ciobanu, M.; Ivan, M. Some geometric aspects in the theory of Lotka-Volterra system. In Proceedings of the 11th WSEAS International Conference on Sustainability in Science Engineering, Timisoara, Romania, 27–29 May 2009; pp. 91–97.
24. Aron, A.; Girban, G.; Kilyeni, S. A Geometric Approach of a Battery Mathematical Model for On-Line Energy Monitoring. In Proceedings of the 2011 IEEE EUROCON-International Conference on Computer as a Tool, Lisbon, Portugal, 27–29 April 2011.
25. Puta, M.; Pop, C.; Danaiasa, C.; Hedrea, C. Some geometric aspects in the theory of Lagrange system. *Tensor* **2008**, *69*, 83–87.
26. Gumral, H.; Nutku, Y. Poisson structure of dynamical systems with three degrees of freedom. *AIP J. Math. Phys.* **1993**, *34*, 5691–5721. [[CrossRef](#)]
27. Gonzalez, G.A.; Nielsen, C.; Bortoff, Z. Attractivity of Unstable Equilibria for a Controlled Chen System via Small Output Feedback. *Chaos Solitons Fractals* **2022**, *164*, 112642. [[CrossRef](#)]
28. Ren, H.-P.; Tian, K.; Grebogi, C. Topological horseshoe in a single-scroll Chen system with time delay. *Chaos Solitons Fractals* **2020**, *132*, 109593. [[CrossRef](#)]
29. Qin, W.-X.; Chen, G. On the boundedness of solutions of the Chen system. *J. Math. Anal. Appl.* **2007**, *329*, 445–451. [[CrossRef](#)]
30. Alvarez-Ramirez, J.; Cevantes, I.; Femat, R. An equilibrium point stabilization strategy for the Chen system. *Phys. Lett. A* **2004**, *326*, 234–242. [[CrossRef](#)]
31. Hu, H.; Liu, L.; Ding, N. Pseudorandom sequence generator based on the Chen chaotic system. *Comput. Physics Commun.* **2013**, *184*, 765–768. [[CrossRef](#)]
32. Cheng, Z. Anti-control of Hopf bifurcation for Chen's system through washout filters. *Neurocomputing* **2010**, *73*, 3139–3146. [[CrossRef](#)]
33. Chowdhury, M.S.H.; Hashim, I. Application of multistage homotopy-perturbation method for the solutions of the Chen system. *Nonlinear Anal. Real World Appl.* **2009**, *10*, 381–391. [[CrossRef](#)]
34. Alomari, A.K.; Noorani, M.S.M.; Nazar, R. Adaptation of homotopy analysis method for the numeric-analytic solution of Chen system. *Commun. Nonlinear Sci. Numer. Simulat.* **2009**, *14*, 2336–2346. [[CrossRef](#)]
35. Liu, Y.; Zhu, J.; Ding, D. Adaptive synchronization of Chen chaotic system with uncertain parameters. *J. China Univ. Posts Telecommun.* **2007**, *14*, 103–105. [[CrossRef](#)]
36. Al-sawalha, M.M.; Noorani, M.S.M. A numeric-analytic method for approximating the chaotic Chen system. *Chaos Solitons Fractals* **2009**, *42*, 1784–1791. [[CrossRef](#)]
37. Noorani, M.S.M.; Hashim, I.; Ahmad, R.; Bakar, S.A.; Ismail, E.S.; Zakaria, A.M. Comparing numerical methods for the solutions of the Chen system. *Chaos Solitons Fractals* **2007**, *32*, 1296–1304. [[CrossRef](#)]
38. Park, J.H.; Lee, S.M.; Kwon, O.M. Dynamic controller design for exponential synchronization of Chen chaotic system. *Phys. Lett. A* **2007**, *367*, 271–275 [[CrossRef](#)]
39. Wang, Y.; Guan, Z.; Wang, H.O. Feedback and adaptive control for the synchronization of Chen system via a single variable. *Phys. Lett. A* **2003**, *312*, 34–40. [[CrossRef](#)]
40. Marinca, V.; Herisanu, N.; Bota, C.; Marinca, B. An optimal homotopy asymptotic method applied to the steady flow of a fourth grade fluid past a porous plate. *Appl. Math. Lett.* **2009**, *22*, 245–251. [[CrossRef](#)]
41. Marinca, V.; Herisanu, N. *Nonlinear Dynamical Systems in Engineering*; Springer: Berlin/Heidelberg, Germany, 2011.
42. Marinca, V.; Herisanu, N. *The Optimal Homotopy Asymptotic Method: Engineering Applications*; Springer: Berlin/Heidelberg, Germany, 2015.
43. Liang, X.; Qi, G. Mechanical analysis of Chen chaotic system. *Chaos Solitons Fractals* **2017**, *98*, 173–177. [[CrossRef](#)]
44. Ariesanu, C.P.; Petrisor, C. A geometric approach of the Chen's system. *IFAC Proc. Vol.* **2012**, *45*, 288–292. [[CrossRef](#)]
45. Zhou, T.; Tang, Y.; Chen, G. Chen's attractor exists. *Int. J. Bifurcat. Chaos* **2004**, *14*, 3167–3177. [[CrossRef](#)]
46. Daftardar-Gejji, V.; Jafari, H. An iterative method for solving nonlinear functional equations. *J. Math. Anal. Appl.* **2006**, *316*, 753–763. [[CrossRef](#)]

Disclaimer/Publisher's Note: The statements, opinions and data contained in all publications are solely those of the individual author(s) and contributor(s) and not of MDPI and/or the editor(s). MDPI and/or the editor(s) disclaim responsibility for any injury to people or property resulting from any ideas, methods, instructions or products referred to in the content.